


Article

Highly Stable and Nontoxic Lanthanum-Treated Activated Palygorskite for the Removal of Lake Water Phosphorus

Bhabananda Biswas ^{1,2,3,*}  and Ravi Naidu ^{2,3}¹ Future Industries Institute, UniSA STEM, University of South Australia, Mawson Lakes, SA 5095, Australia² Cooperative Research Centre for Contamination Assessment and Remediation of the Environment, Callaghan, NSW 2308, Australia; Ravi.Naidu@newcastle.edu.au³ Global Centre for Environmental Remediation, The University of Newcastle, Callaghan, NSW 2308, Australia

* Correspondence: Bhabananda.Biswas@newcastle.edu.au

Abstract: Nutrient pollution of surface water, such as excess phosphate loading on lake surface water, is a significant issue that causes ecological and financial damage. Despite many technologies that can remove available phosphate, such as material-based adsorption of those available phosphate ions, the development of a material that can trap them from the surface water is worth doing, considering other aspects. These aspects are: (i) efficient adsorption by the material while it settles down to the water column, and (ii) the material itself is not toxic to the lake natural microorganism. Considering these aspects, we developed a trace lanthanum-grafted surface-modified palygorskite, a fibrous clay mineral. It adsorbed a realistic amount of phosphate from the lake water (typically 0.13–0.22 mg/L). The raw and modified palygorskite (Pal) includes unmodified Australian Pal, heated (at ~400 °C) Pal, and acid (with 3 M HCl)-treated Pal. Among them, while acid-treated Pal grafted a lower amount of La, it had a higher adsorption capacity (1.243 mg/g) and a quicker adsorption capacity in the time it took to travel to the bottom of the lake (97.6% in 2 h travel time), indicating the adsorption role of both La and clay mineral. The toxicity of these materials was recorded null, and in some period of the incubation of the lake microorganism with the material mixture, La-grafted modified clays increased microbial growth. As a total package, while a high amount of La on the already available material could adsorb a greater amount of phosphate, in this study a trace amount of La on modified clays showed adsorption effectiveness for the realistic amount of phosphate in lake water without posing added toxicity.

Keywords: modified clays; Australian palygorskite; phosphate adsorption; biocompatible material

Citation: Biswas, B.; Naidu, R. Highly Stable and Nontoxic Lanthanum-Treated Activated Palygorskite for the Removal of Lake Water Phosphorus. *Processes* **2021**, *9*, 1960. <https://doi.org/10.3390/pr9111960>

Academic Editor: Enrico Marsili

Received: 9 October 2021

Accepted: 29 October 2021

Published: 2 November 2021

Publisher's Note: MDPI stays neutral with regard to jurisdictional claims in published maps and institutional affiliations.



Copyright: © 2021 by the authors. Licensee MDPI, Basel, Switzerland. This article is an open access article distributed under the terms and conditions of the Creative Commons Attribution (CC BY) license (<https://creativecommons.org/licenses/by/4.0/>).

1. Introduction

Nutrient pollution, in particular excess phosphorus (P) accumulation in lake surface water, is a serious problem for water quality, ecosystems, and healthy food chains [1]. One of the consequences is the algal bloom caused by the available form of P such as phosphate in the surface water [2]. Burying down the excess P from the surface water to the deep water of the lake could mitigate the eutrophication problem, however, often is not technically viable to do so.

Using a low-cost material with sufficient binding capacity to phosphate and fast sedimentation tendency could help mitigate P pollution of the lake surface water. Modified clays became promising material technologies to serve the same purpose [3]. Among those modified clays, lanthanum (La)-treated clay minerals have been deemed to be effective to remove P from its available form into a precipitated complex. In this instance, the mechanism related to the adsorbent–adsorbate interaction prevails due to the strong affinity of La compounds to P compounds [4,5]. However, when the clay is treated with La ions, it could also raise toxicity concerns caused by the lanthanum [6]. This is due to the leaching of La from the composite material back to the water body, depending on the water and material chemistry [7,8].

Therefore, scope exists to synthesise such a modified clay where La does not pose an ecotoxicity risk but remains effective for removing phosphate from the water surface, most favourably through adsorption of P followed by settling to the sediment floor. As reported, the smectite group of clay minerals, such as montmorillonite, has been commonly used to produce functional material for P adsorption [9,10]. Other low-cost clay minerals with good biocompatibility could also make new and sustainable composite material for the removal of P from surface waters, such as from open lake water.

In this study, we used an Australian fibrous clay mineral identified as palygorskite (also known as attapulgite) to be grafted with a low dosage of La, which could be efficient for the removal of phosphate and total phosphorous available in the real lake water. In the literature, few studies reported the application of La-treated palygorskite (Pal) for the adsorption of phosphate from the water [11,12]. However, the toxicity of the whole composite material and the adsorption capacity of materials during the sinking time is important in terms of safe use of material. These are critical gaps that need to be addressed by research experiments using real lake water, such as that used in the present study. Furthermore, the mode of functionalisation of Pal prior to the La treatment is also another critical aspect that could tailor the overall La-mediated phosphate adsorption in the lake water. Considering that, while raw Pal is the fibrous non-expandable phyllosilicate mineral [13], here we used two modified Pals obtained after moderate thermal and acid treatment. Therefore, the effect of various pre-treatment of Pal on the La grafting and thereafter adsorption of phosphate was also tested in this study.

2. Materials and Methods

2.1. Materials and Reagents

An Australian palygorskite (Pal) supplied by Hudson Resource Ltd., Australia (geological source: Western Australia, Cation Exchange Capacity 19.0 cmol[P+]/kg) was used as the parent clay mineral for its further modifications. The Pal was activated in two ways: (i) thermal energy at 400 °C for 2 h, and (ii) acid (3M hydrochloric acid, HCl) treatment for 45 min. The resulting materials are known as Pal400, and Pal3M, respectively, while the unmodified Pal is referred to as PalU. The detailed method of material preparation was previously reported by Biswas, et al. [14] for Pal400 and Biswas, et al. [15] for Pal3M. While La was purchased from Sigma-Aldrich, Australia as $\text{LaCl}_3 \cdot 7\text{H}_2\text{O}$ reagent grade, the P stock was prepared using KH_2PO_4 reagent grade (LabServ Australia). For the pH adjustment, 0.1 M of HCl or sodium hydroxide (LabServ Australia) was used. Where applicable we used Milli-Q (MQ) water (resistivity 18.2 $\Omega \cdot \text{cm}$).

2.2. La Modification of Activated Palygorskite

The activated Pal was further modified with LaCl_3 where La^{3+} equivalent was added to the clay with 2% La^{3+} /clay ratio (w/w). The fraction of solid to liquid was 10%. Using the drop-wise acid or alkali, the pH was adjusted to 6.0 ± 0.4 (pH meter: SmartCHEM, TPS Australia) before continuous stirring of the mixture at 1500 rpm for 2 h at 60 °C (Magnetic stirrer: IKA[®] C-MAG HS series 7, Germany). The stirring was furthered for another 12 h without heat followed by additional 12 h ageing without heat or stirring. The powdered materials were recovered after freeze-drying (ModulyoD, USA) and hand-grinding using an agate-mortar. The La-grafted clays were then calcinated at 250 °C for 2 h under N_2 flow followed by their cooling under vacuum desiccation [16]. As preliminary studies, we tested whether there was any significant difference between calcinated and non-calcinated composites. Since calcination did not change materials' crystallinity, rather slightly improved the positive surface charge of the composite (Supplementary Information, SI Figures S1 and S2), additional material characterisations and adsorption experiments were carried out using only calcinated materials. Previous studies also suggested that calcinated La-treated clays could increase the efficiency of the binding sites for the phosphate in an aqueous solution, while the material stability was achieved [11,17]. The materials were stored under vacuum at room temperature for characterisation and

adsorption experiments. For the identification, the La-modified material was named after their functionalisation such as La@PalU, La@Pal400, and La@Pal3M.

2.3. Characterisation of La-Treated Palygorskite Materials

For the confirmation of the presence of La on the clays, we used inductively coupled plasma mass spectrometry (ICP-MS) (Agilent Technologies, USA) of microwave-assisted acid-digested sample solution (digestion method: EPA 3051A) [18]. In brief, a 5 mL mixture of concentrated nitric and hydrochloride acids (3:1) was added to 0.1 g of solid sample in a digestion vessel to complete a thermal and pressure cycle in a CEM MARS 6 Microwave Digestion System (Temperature 175 °C with a hold time of 10 min). The extracted supernatant was then analysed by ICP-MS against an internal standard of iridium isotope (^{191}Ir , High-Purity Standard, USA), while certified La standard (High-Purity Standard, USA) was used to quantify the analytes (detection limit = 0.05 ppb). We also used raw Pal in the same process and tested if there was any background residual La. We also used X-ray diffraction (XRD) (PANalytical Empyrean, The Netherlands) of the powdered samples to determine the materials' crystallinity properties with the phase suggested by the X'pert HighScore software [19]. The surface charge in the form of Zeta (ζ) potential was also measured from the 0.05% aqueous (MQ water) solution of materials using Malvern-Zeta sizer Nano ZS at its inherent pH. Scanning microscopic images coupled with Energy-dispersive X-ray spectroscopy (EDS) profiling were obtained from 2 nm thick platinum-coated samples using Zeiss Merlin FEG SEM with SDD EDS (Germany). The high-resolution X-ray photoelectron spectroscopy (XPS) was also performed for the La, O, and C region of the material using an Al X-ray sourced XPS (Kratos AXIS Ultra DLD, UK), which was processed against C 1s calibration at 284.8 eV and modelled with CasaXPS software 2.3.19PR1.0 [20].

2.4. Phosphate Adsorption by Modified Clays

We took several adsorption approaches to simulate P removal from lake water. First, we prepared a P solution (1000 mg/L) using tap water with a pH of ~6.0, considering that this pH was commonly observed in the studied lake water. At this stage, keeping replication, we conducted single concentration adsorption (~7 mg/L of PO_4^{3-} equivalent) at 5 mg/mL material loading to the 20 mL of P solution for the comparison of ranges of materials. The PO_4^{3-} was detected using ion chromatography (Dionex™ Aquion™, USA) against Ion Chromatography Anion Standard solution (Supelco®, Merck, Australia).

Based on the obtained adsorption capacity, an adsorption isotherm experiment was further conducted using selected adsorbents where 1–30 mg/L of PO_4^{3-} equivalent solution was used. We then verified the materials' performance against total phosphorus in the solution by using multiple concentrations of total P solution (1–50 mg/L of total P equivalent). In this case, the total P was measured using an inductively coupled plasma optical emission spectrometer (ICP-OES) (Agilent Technologies, USA). It is worth noting that this excess amount of P is unrealistic for most of the eutrophication lake water [2], but here we used this range of concentration to reveal the adsorption capacity of the selected materials. Triplication was maintained for all these adsorption experiments.

In eutrophication or algal bloom potential lakes, the P concentration generally varies between 0.13 and 0.22 mg/L [2]. We also, therefore, experimented using real lake water where the P was spiked to obtain a realistic concentration (0.5 mg/L) of total P in duplicate along with keeping negative control (without any P spiking) as well. This would further confirm the material performance in natural lake water interference. In this case, we collected surface water (3 random spots, 0–15 cm, pH ~6.0) in a sterile dark container from a lake located in Mawson Lakes, South Australia on a sunny early afternoon. The replicated samples were mixed in a sterile container and stored in a 4 °C room overnight, undisturbed, to allow the settling of debris and larger particles before using for the adsorption experiment.

2.5. Material Stability, Microbial Toxicity and Settling Capacity of Materials

The leaching of La from modified palygorskite was measured from the aqueous phase of the equilibrium state of phosphate adsorption reaction conducted in MQ and lake water. The MQ water and the phosphate stock solution were kept as the control. Furthermore, XPS analysis was performed on the spent materials (post-P-adsorbed pellet) to observe any change in the state of the La compound.

To test the biocompatibility of the modified materials, bacterial growth was monitored from the material-mixed culture media. The clean water was taken to mix material at its 5 mg/mL concentration (*w/v*) and incubated under continuous shaking at 150 rpm at room temperature. With the progress of time, the colony-forming unit (CFU) method was applied to count the heterotrophic bacteria which was cultivated on an R2A agar plate from the sub-sample of the material-amended liquid culture [21]. While the pure lake water represents the positive control, the material-mixed sterile lake water serves as the negative control for detecting the presence of any potential material-borne bacteria (Supplementary Information, SI Figure S3). The CFU was counted on 3–5 days after placing it on an agar plate. In the case of microbe-mediated leaching of La from the composite materials, we also detected La at the end of 340 h of the culture period.

The settle capacity of the material (1 mg/mL in lake water in 25 mm wider confined column) was also tested following a modified method of Torfs, et al. [22]. Briefly, the material was mixed in 50 mL of lake water in a 50 mL glass cylinder and the enclosed container was shaken well. Then in a time scale, the top 20 mL was withdrawn undisturbed (~top 5 cm) for the turbidity measurement using a turbid meter (HACH, model: 2100N, Australia). The visual snap of the water column of the cylinder was also recorded on a digital camera. Following the above procedure, once the plateau of the particle settling time was achieved, another similar settling set-up was installed for the measurement of the total P from the top 5 cm of the water column. This provided an estimation of the real-time P removal capacity in the course of the material's travel down to the bottom of the cylinder.

2.6. Statistical Analysis and Graphical Presentation

Where applicable, IBM® SPSS® Statistics (version 26) was used to perform Analysis of variance (ANOVA) among the treatments. For all figure and graphical presentations, Microsoft products, including Excel and its add-in, such as Solver (version 2017), and PowerPoint (version 2017) were used.

3. Results and Discussion

3.1. Characterisation of Materials

3.1.1. Crystalline Phase and Elemental Composition of Modified Materials

The unmodified Pal shows its characteristic diffraction peaks at $2\theta = 8.48^\circ$ (d_{110}) and $2\theta = 19.96^\circ$ (d_{121}) and with an impurity of quartz and carbonate (e.g., dolomite) at $2\theta = 26.66^\circ$ and 30.9° , respectively (Figure 1A). While the raw Pal was heated at 400°C , it had a little change, such as a slight decrease in the intensity attributed to the Pal intensity (Figure 1B). On the other hand, in the moderately strong acid treatment (3M HCl for 45 min), raw Pal could eliminate or reduce few types of impurities, such as carbonate materials (Figure 1C). Details of the characterisation of these two modified Pal is out of the context of this study but can be read from our previous published studies [14,15,23].

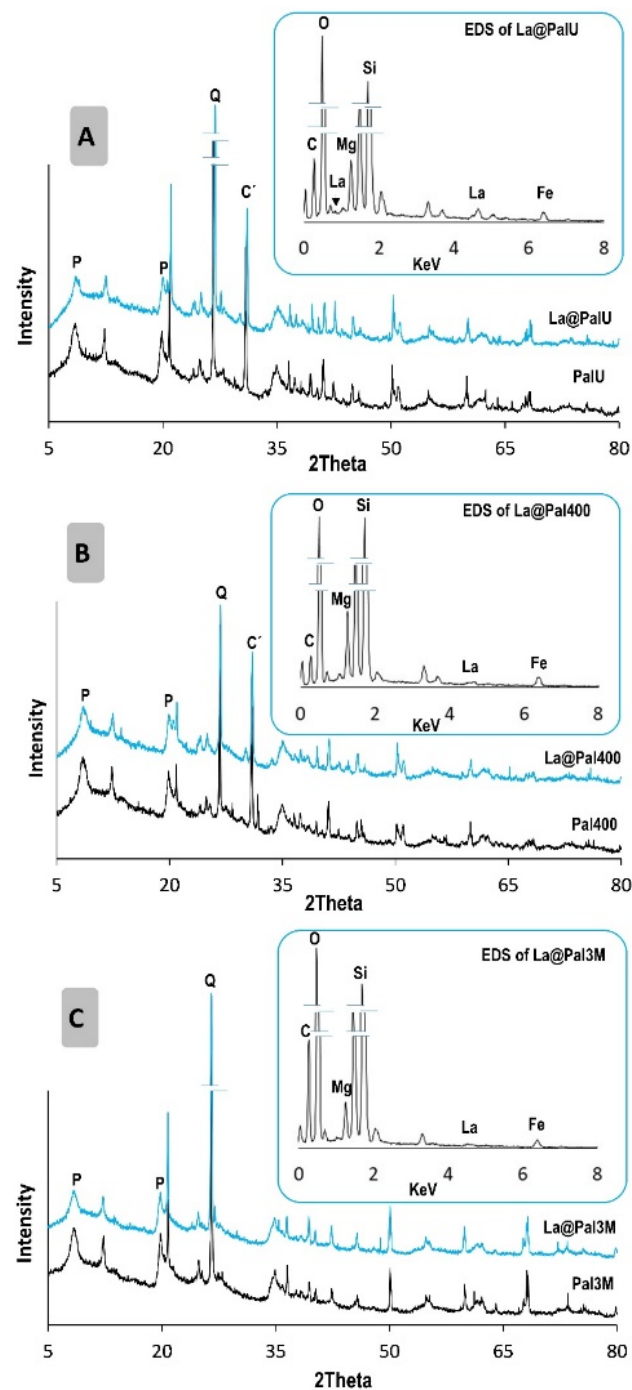


Figure 1. XRD of raw and modified palygorskite. (A) PalU and its modifications; (B) Pal400 and its modifications; and (C) Pal3M and its modifications. In the peak annotation: P = palygorskite, Q = quartz, and C' = carbonate material. The EDS of only PalU is provided as the Supplementary Information SI Figure S4.

Such modifications add some surface properties, including the rise of alkaline sites on Pal by the heat (≤ 400 °C) [24] or removing organic matter and other impurities, which additionally help to increase the surface area in the case of acid treatment [15,25]. While these materials were treated with La solution, there was no strong evidence of any new mineral phase potentially introduced as a result of the grafting of La. This non-crystallinity behaviour of La on materials was also reported elsewhere [26,27]. However, a trace of La was detected as evidence of EDS spectra of La α signature in the region of KeV of 4.6. In this

case, a low amount of La was detected for La@Pal3M compared to the other two composites in concert with the absolute detection presented in Figure 1 (inset of Figures 1 and S4).

3.1.2. La Retention on Palygorskite and Modified Palygorskite

Lanthanum was loaded on the material variably depending on the type of materials applied. For example, the absolute extraction of La from La@PalU showed 16.60 ± 0.15 mg La per g material, as an equal yield to that from La@Pal400. However, they differed significantly from La@Pal3M (7.20 ± 0.13) ($p < 0.05$). We matched these values with the unbound La concentration present in the supernatant upon the adsorption reaction was completed. They were not different within each material, confirming only a clay-La interaction during a reaction without any significant loss on glassware (Figure 2).

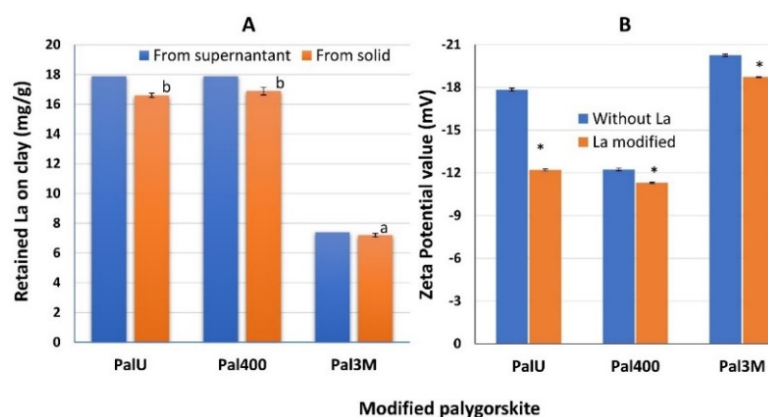


Figure 2. Amount of La on the raw and modified palygorskite (A). Only the solid samples were extracted in duplicate showing mean with the column bar and standard deviation with the error bar. The different letters on the top of the bar indicate a significant difference at 95% level of confidence. Also, the zeta potential of material before and after La treatment (B). The star (*) represents that the zeta value changes significantly from its parent material after La treatment.

The La concentration (1.79 mg/mL, see Material and Methods) was efficient for PalU and Pal400 which utilised 100% of the given amount of La, but it was only 41.32% by Pal3M. While acid treatment increased the specific surface area of raw Pal [15,28], a comparatively low amount of La adsorbed on the Pal3M might not be related to the surface area, rather ionic attraction where pH might have played a key role. A pH ~6 or above leads to the formation of La compounds, such as carbonate or bi-carbonate complexes, over ionic La [6]. In this case, Pal3M might have influenced lowering the initially set pH (~6) during the La adsorption reaction where only ionic La was allowed to be adsorbed onto the functional sites of clay. The significant positive change in the surface charges of the composite once La was incorporated also showed the effectiveness of clay modification of a given amount of lanthanum solution (Figure 2B). In these cases, PalU had a ζ -value of -17.83 , which reduced to -12.43 for La@PalU, while other modified Pals (Pal400 and Pal3M) changed variably lower than this. A load of positively charged La increased positive charge on the surface of clay used [29].

3.1.3. Microscopic Images of Modified Materials and the Elemental State of La

The raw Pal was fibrous elongated particles where a trace of kaolin clay was also present in the bulk (Supplementary information, SI Figure S4). While the pre-functionalised Pal such as Pal400 and Pal3M affected the morphology of raw Pal such as aggregation [15,23], the La treatment and subsequent moderate calcinated heat did not alter the fibrous morphology of the materials any degree more (Figure 3). SEM did not show any material formation of La on the surface of the functionalised Pal that is in support of XRD non-crystalline nature of La presence, however, the XPS unveils grafting of La on them (Figure 3). The spin-orbit component of La_{3d5/2} region at the eV 830–840 represents the presence of La in

the form of its oxides, hydroxides, and oxycarbonate [30]. Further, the multiplet of this region likely indicates La compounds such as La carbonate, because the difference compared to the multiplet ($\Delta E/eV$) is closer to 3.5 [30,31]. In the additional analysis of the O 1s and C 1s regions, the presence of oxycarbonate form of La compounds on the clay surface was evidenced as the spike of O 1s peak at $\sim 532\text{--}533.6$ eV in concert with the appearance of C 1s peak at ~ 290 eV (see Supplementary Information SI Figures S5 and S6) [31].

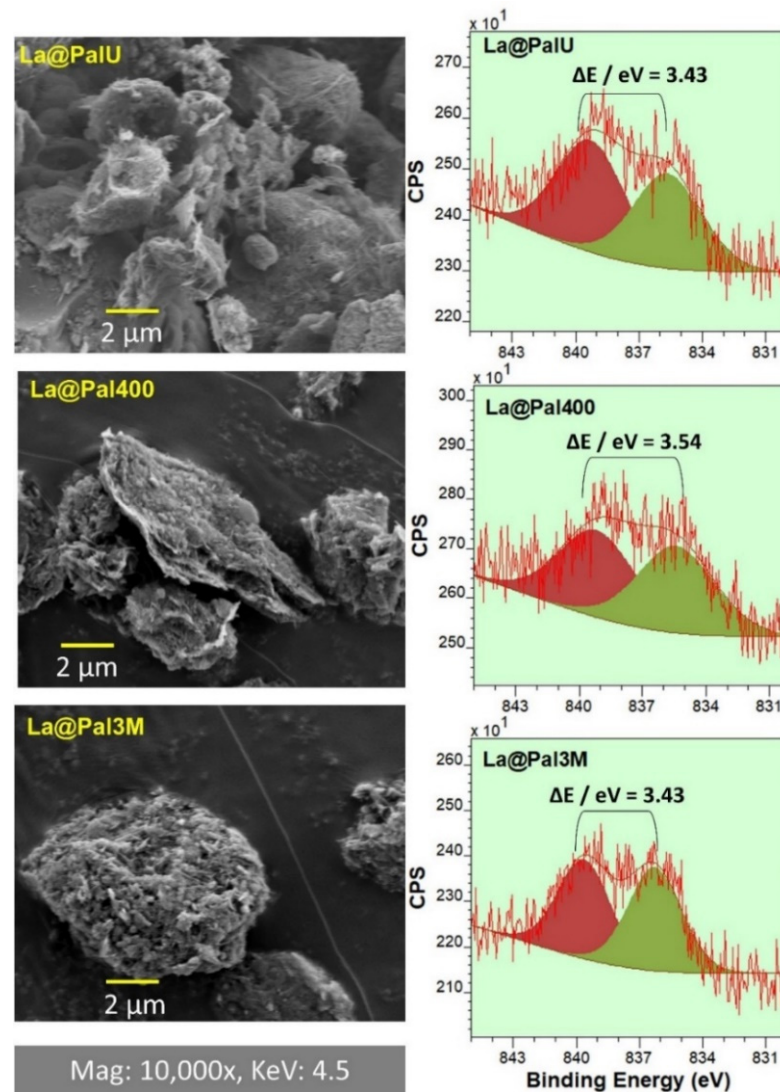


Figure 3. SEM images of La-functionalised palygorskite materials. Microscopic images (SEM and TEM) of the raw palygorskite are provided as the Supplementary Information SI Figure S4. High-resolution XPS and model fitting of La signature spectra are in the right column of the figure.

3.2. Removal of Phosphate from Tap and Lake Water

Figure 4 shows that the La treatment of activated Pal significantly improved the adsorption efficiency of phosphate from the tap water-spiked solution ($p < 0.05$). Among the La-treated materials, the order of effective adsorbent was La@Pal400 ($92.42 \pm 0.34\%$ removal of given phosphate) \geq La@PalU ($88.22 \pm 8.44\%$) $>$ La@Pal3M ($75.75 \pm 2.09\%$).

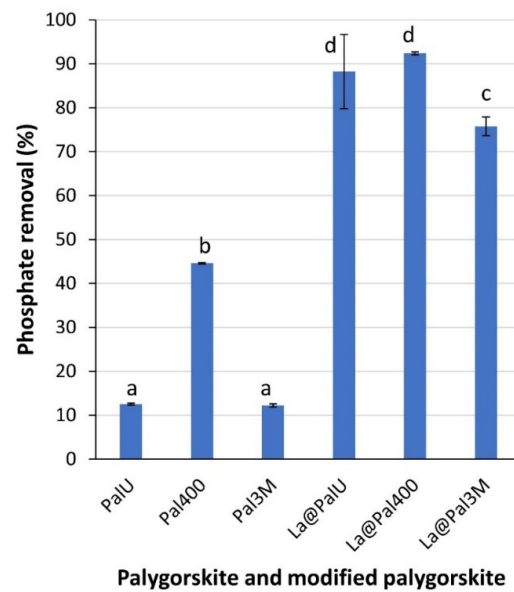


Figure 4. The adsorption of single concentration phosphate by various activated and modified palygorskite materials. The different letters on the top of the bar indicate a significant difference at a 95% level of confidence.

Following this single concentration adsorption experiment, we selected the top three materials and carried out multiple concentrations of phosphate ion to determine the adsorption capacity of the given materials. We performed commonly applied adsorption isotherm models using non-linear Langmuir [32], Freundlich [33], and Langmuir-Freundlich interaction (also known as Sip's) equations (Table 1 and Figure 5).

Table 1. Model parameters of adsorption isotherm of phosphate by the modified palygorskite materials.

Model	Equation *	Parameters	La@PalU	La@Pal400	La@Pal3M
Langmuir	$q_e = \frac{q_{max}K_L c_e^n}{1+K_L c_e^n}$	q_{max} (mg/g)	1.319	1.013	1.290
		K_L (L/mg)	3.236	11.602	1.646
		R^2	0.907	0.350	0.977
		RMSE	0.099	0.180	0.0462
Freundlich	$q_e = K_F C_e^{\frac{1}{n}}$	K_F (mg/g)	0.924	0.891	0.790
		n (dimensionless)	5.841	20.838	4.752
		R^2	0.795	0.146	0.840
		RMSE	0.146	0.206	0.123
Langmuir-Freundlich (Sip's)	$q_e = \frac{q_{max}K_{Sip}c_e^n}{1+K_{Sip}c_e^n}$	q_{max} (mg/g)	1.227	1.002	1.243
		K_{Sip}	3.024	3.697	1.710
		n (dimensionless)	2.095	24.364	1.179
		R^2	0.947	0.875	0.982
		RMSE	0.075	0.079	0.042

* q_e is the adsorbed amount at equilibrium (mg/g) while c_e is the concentration of adsorbate at equilibrium (mg/L); for Langmuir and Sips, q_{max} is the maximum monolayer adsorption capacity (mg/g), K_L or K_{Sip} is the constant related to the affinity of adsorbate to the material (L/mg), while for Sips and Freundlich, n (dimensionless) is the constant; for the Freundlich model, K_F is the Freundlich constant related to adsorption capacity [34]. RMSE = root mean square error. The shaded values indicate that they are not fitted to the corresponding model. An explanation is in the main text.

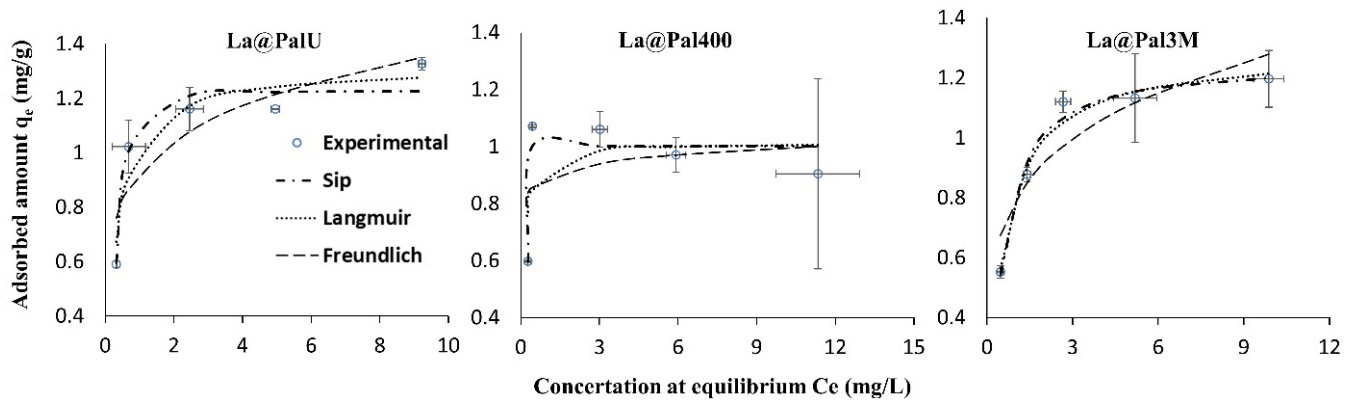


Figure 5. The adsorption of phosphate on modified palygorskite and various models to predict the adsorption capacity of the material in the given conditions.

None of the materials exhibited adsorption mechanisms related to the Freundlich isotherm perfectly. However, they fitted to the Sip's isotherm, while to the Langmuir isotherm for only La@PalU and La@Pal3M (Figure 5 and Table 1). This indicates that the adsorption of phosphate tends to occur mainly on the monolayer arrangement of the binding sites of these composites. A sharp increase in adsorption in the low concentration of phosphate solution followed by a rapid decline of such capacity made the La@Pal400 unfit with the Langmuir model as well (Figure 5). Indeed, an unusually large n value for La@Pal400 ($n \sim 24.364$) was derived by the Sip's model as a result of its competency only in low concentration of adsorbate [34]. The Sips model essentially utilises the Freundlich principle at a low concentration of adsorbate and Langmuir at higher ends [35]. Considering high R^2 and low error (RMSE), the Langmuir–Freundlich (Sips) interaction model fitted the best for all composites where maximum adsorption capacity q_{max} was in the order of La@Pal3M (1.243 mg/g) > La@PalU (1.227 mg/g) > La@Pal400 (1.002 mg/g).

Using the same phosphate solution, we also detected total P and calculated the removal efficiency (%) by the materials in various initial concentrations of P solution. Note that removal efficiency was the preliminary indication of the performance of any given material where the mass of adsorbent is not considered [34]. However, we used an equal amount of adsorbent, using a five decimal point sensitive electric balance to be as precise as possible. In the case of removal efficiency at 1 mg/L of P solution, both La@PalU and La@Pal400 materials removed >99% of P from the solution, while La@Pal3M was effective with only about ~89% adsorption capacity. These efficiencies dropped significantly while the initial concentration of adsorbate increased (Table 2). In concert with the adsorption isotherm of phosphate (Figure 5), it is apparent that La@Pal400 was incapable of adsorbing P when at a high concentration of adsorbate (Table 2).

3.3. Material Stability, Binding Mechanism, Biocompatibility and Settling

3.3.1. Leaching of La from the Materials

During P adsorption in tap water, the leaching of La of the material was highly insignificant, accounting 0.0001–0.0208% from the composite. Among them, PalU showed the best anti-leaching properties ($1.03 \times 10^{-4} \pm 7.08 \times 10^{-5}\%$) followed by Pal400, and Pal3M (Table 3). While in the lake water, the La leaching potential was also minimised by the material stability (Table 3), even by the available bacterial intervention.

Table 2. Removal capacity of selective adsorbents in various initial concentration of P in aqueous solution.

Materials	Initial Concentration P (mg/L, Nominal)	Removal Capacity (%)
La@PalU	1	99.77 ± 0.00
	5	41.45 ± 8.26
	20	9.17 ± 0.95
	50	1.46 ± 0.98
La@Pal400	1	99.80 ± 0.02
	5	40.75 ± 2.00
	20	8.25 ± 0.50
	50	0.38 ± 0.53
La@Pal3M	1	89.07 ± 2.72
	5	47.88 ± 0.80
	20	14.60 ± 0.57
	50	6.68 ± 2.40

Table 3. Leaching of grafted La from the modified palygorskite during P adsorption reaction.

Materials	% Loss of Grafted La in	
	MQ Water	Lake Water
La@PalU	$1.03 \times 10^{-4} \pm 7.08 \times 10^{-5}$	$1.64 \times 10^{-3} \pm 7.58 \times 10^{-4}$
La@Pal400	$6.55 \times 10^{-4} \pm 2.75 \times 10^{-4}$	$1.23 \times 10^{-3} \pm 1.05 \times 10^{-4}$
La@Pal3M	$3.94 \times 10^{-3} \pm 1.87 \times 10^{-3}$	$2.51 \times 10^{-3} \pm 1.10 \times 10^{-4}$

The pH plays a critical role in the leaching of La in the aqueous solution, as pH below 4.0 increases such leaching potential [36]. In this study, the tap water, as well as the lake water, had a pH of ~6, which could avoid any pH-induced La leaching from the modified materials.

3.3.2. Potential Binding Mechanism of Phosphate on Materials

The SEM images and XPS profile of post adsorption materials also support the stability of La grafting on the selected functionalised Pal (Figure 6). Neither the fibrous morphology nor the aggregation pattern was changed in the course of the P adsorption reaction. However, in the case of La on the activated Pal, a slight ‘pattern shift’ occurred in the La state as revealed by the eV difference of multiplet splitting of the La3d5/2 region of La in the XPS spectra (Figure 6). These were further supported by changes, such as the minor position shift along with % area of the spectral region of oxycarbonate-denoting O 1s and C 1s XPS peaks (Supplementary Information SI Figures S5 and S6). Without significant leaching of La (Table 3), these changes in the elemental states of oxycarbonates of La might indicate active participation of the La compound in the phosphate adsorption. Indeed, the CO₃²⁻ indicative C 1s peak area at ~290 eV of pre-adsorption material was reduced for post-adsorbed spent material (Supplementary Information SI Figure S6), unveiling a possibility of replacement of CO₃²⁻ by the phosphate molecules during the material–adsorbate interaction [37].

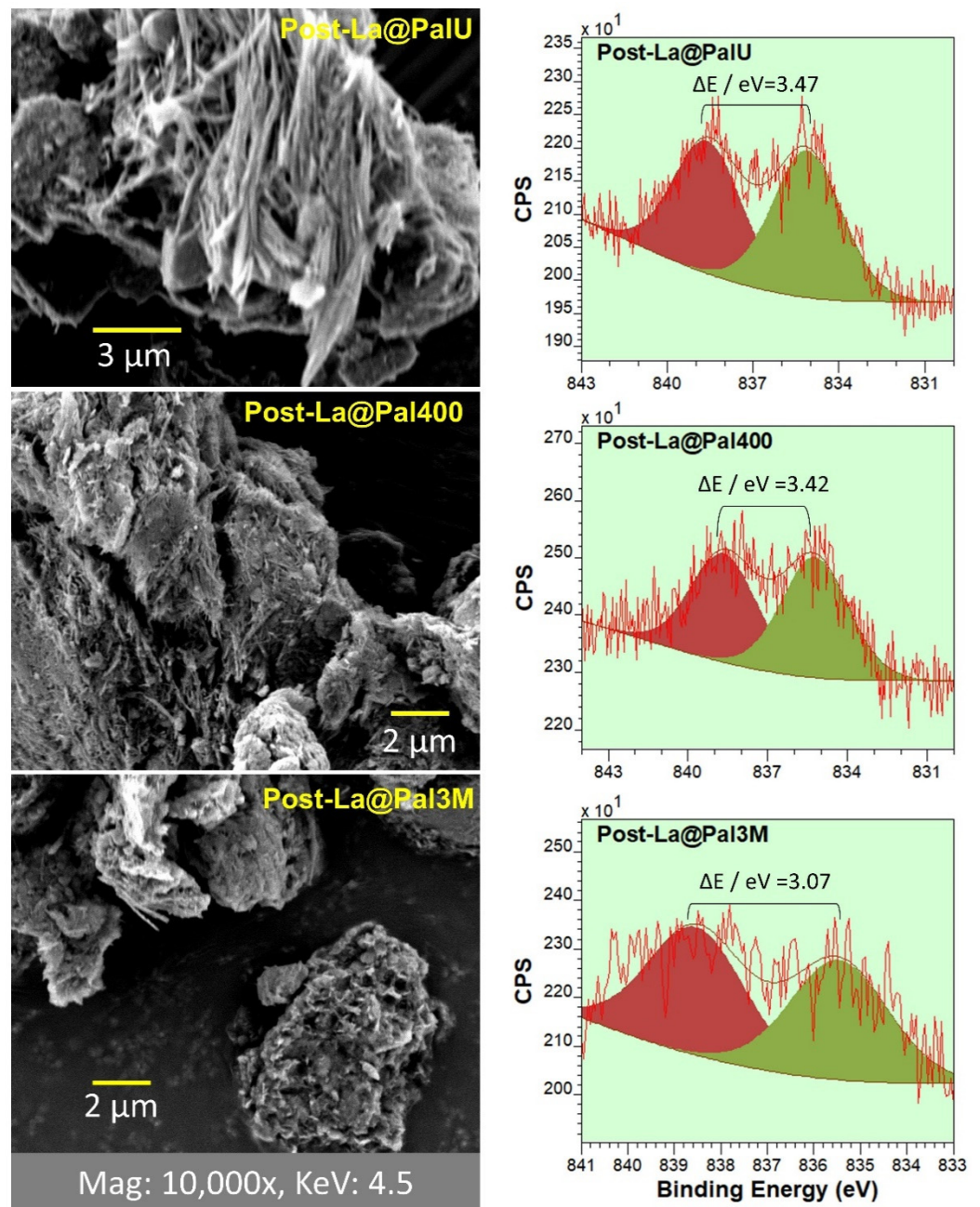


Figure 6. The SEM images of material after P adsorption in MQ water (left column) and the high-resolution XPS of La region of selective spent material of La-modified palygorskite.

3.3.3. Effective Settling and Turbidity of Modified Clays

We also tested the setting capacity of the modified clays. We used the turbidity profile of the water column influenced by the presence of the material. The turbidity of the lake water was ~ 16.6 NTU. The turbidity profile over time also showed that the modified materials had a settling property by ~ 120 min of the initial dispersion of material in the lake water. However, the turbidity of the top later water varied among the materials. For instance, the materials' retention in the upper layer of the water column (5 cm) was longer for LaPalU followed by Lapal400 and LaPal3M (Figures 7 and S7). Interestingly, the quicker settler composite La@Pal3M was more effective to adsorb the low concentration of available phosphorus ($\sim 97.64\%$ of 1 mg/mL loading). While we used real lake surface water, a lanthanum hydroxide-grafted Pal variant showed a similar settling time in deionised water as previously reported [11].

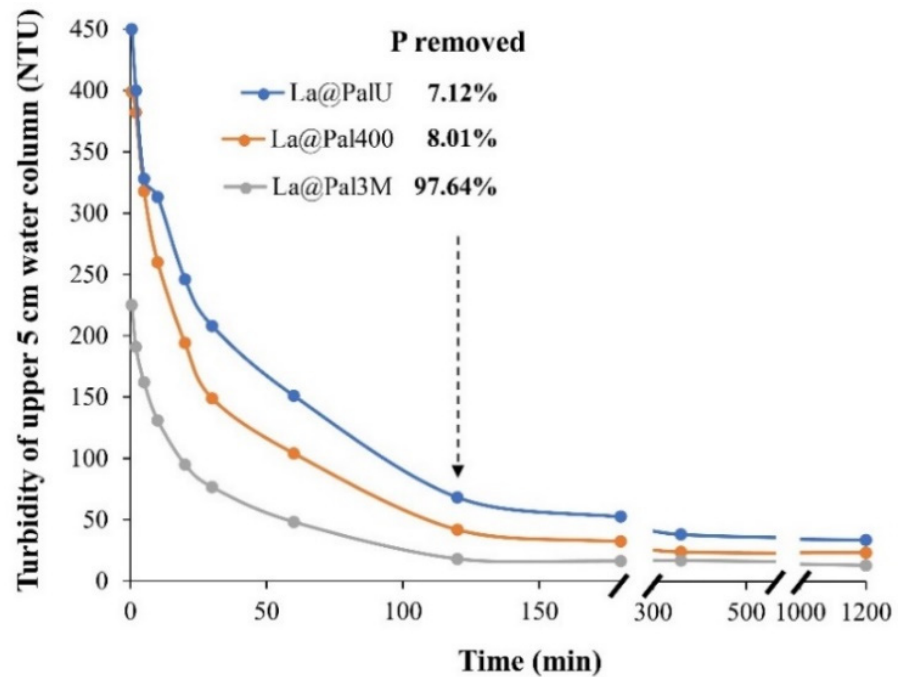


Figure 7. Turbidity measurement of selective materials over a series of times in the water column.

3.3.4. Microbial Toxicity of Modified Clays

The bacterial colony reveals that the La-treated Pal and activated Pal materials were not toxic to the bacteria available in the surface lake water, rather those materials increased microbial growth variably periodically (Figure 8).

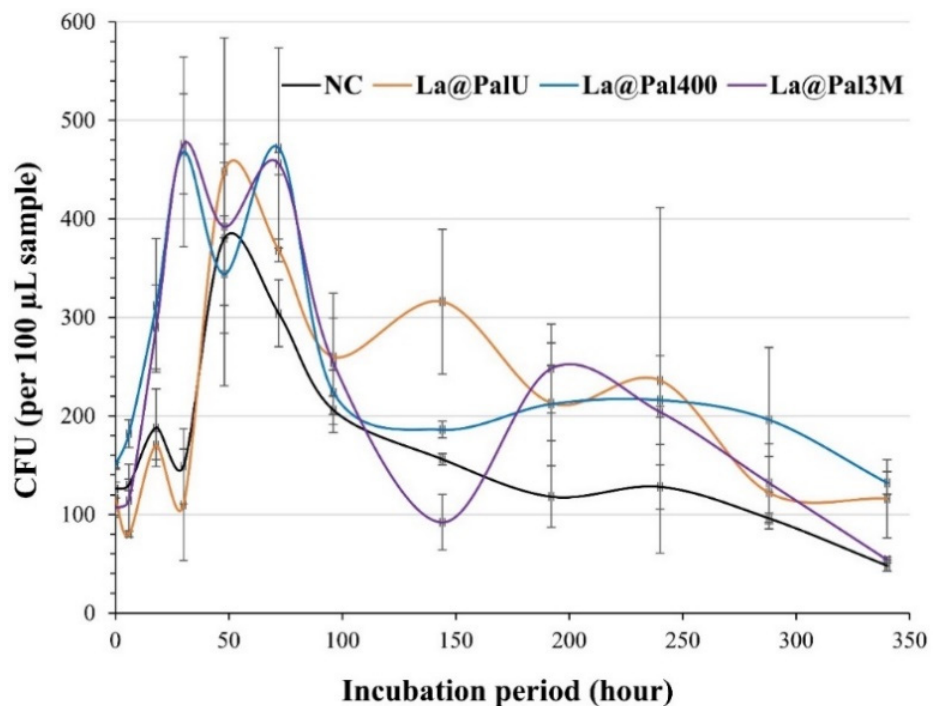


Figure 8. Bacterial growth in control lake water and the presence of various modified palygorskite materials. The growth is presented as the colony-forming unit per 100 μL of the aqueous suspension. NC = no clay (control).

For example, with variability and oscillation in the lag phase, the heterotrophic and only cultivable bacteria of pure lake water grew on agar media to their maximum at ~48 h (380 CFU/100 µL water) followed by a gradual decline. In contrast, La@Pal400 and La@Pal3M-spiked lake water influenced a slightly different growth curve, showing an early maximum of log phase of bacterial growth, resulting in ~468 CFU/100 µL and ~476 CFU/100 µL at around 30 h. The material itself did not contaminate the assessment of CFU as revealed by the sterile lake water bacterial growth (Supplementary Information, SI Figure S3). While free La is toxic to the aquatic (micro)organisms [6], the clay and modified clay-bound La might not be harmful to the bacteria. In the current study, we used 170 rpm shaking of culture flask containing material suspension, which might not be the actual physical water dynamics in lake surface and column, but regardless, it was enough agitation for material particles to contact the suspended bacterial population. As settling time was found to be quick (~2 h) (Figure 7), the early stage of microbial contact to material matters. In this case, no material exhibited any toxicity, a proxy of the CFU count of bacteria (Supplementary Information, SI Figure S8).

4. Cost-Effective Analysis, Implications and Conclusions

We utilised a very mild amount of La to make functionalised Pal clays considering their toxicity, and phosphorus adsorption capacity related to the real lake water guideline values. Compared to other related composites [10–12], the synthesised materials did not show superior adsorption capacity toward the phosphate. However, the low-cost materials were stable and nontoxic while used directly in the lake water. At the current market price, the palygorskite costs USD 0.05–0.5 a kg depending on geological sources, grade and bulking. With this consideration, another two activations, such as heating at 400 °C (2 h) and acid treatment 45 min with 3M HCl, would add a very minimum cost for bulk materials due to the requirement of only a conventional chemical chamber facilities.

Compared to other modified Pals used in this study, the unmodified Pal (PalU) accommodated a higher amount of La on its surfaces which offered adsorption sites for the P. However, in terms of mode of the application such as material spreading on the surface water, La@Pal3M outperformed other materials. Despite that the Pal3M grafted less amount of La than PalU and Pal400 (Figure 3), an equivalent amount of composite performed faster for the adsorption of P during its time travel to the bottom of the lake. It implies that La alone was not the role player, rather the types of activated Pal matter (Figure 9).

We identified a few limitations of this study, such as toxicological assessment using a broader range of toxicity indices (e.g., using other water organisms other than bacteria only) and La concentration and pH-dependent P adsorption analysis. Nevertheless, the current findings will shed light on synthesising minimised La-loaded clay materials that are sufficient to remove a realistic and required amount of P from real lake water. Indeed, Zhao et al. [2] reported that total phosphorus concentration at 0.13–0.22 mg/L in lake water was the threshold to trigger algal bloom. Therefore, in this study, using such a low concentration of phosphorus in tap and real lake water would be relevant in developing useful material such as trace La-grafted clay for direct use on a lake surface water.

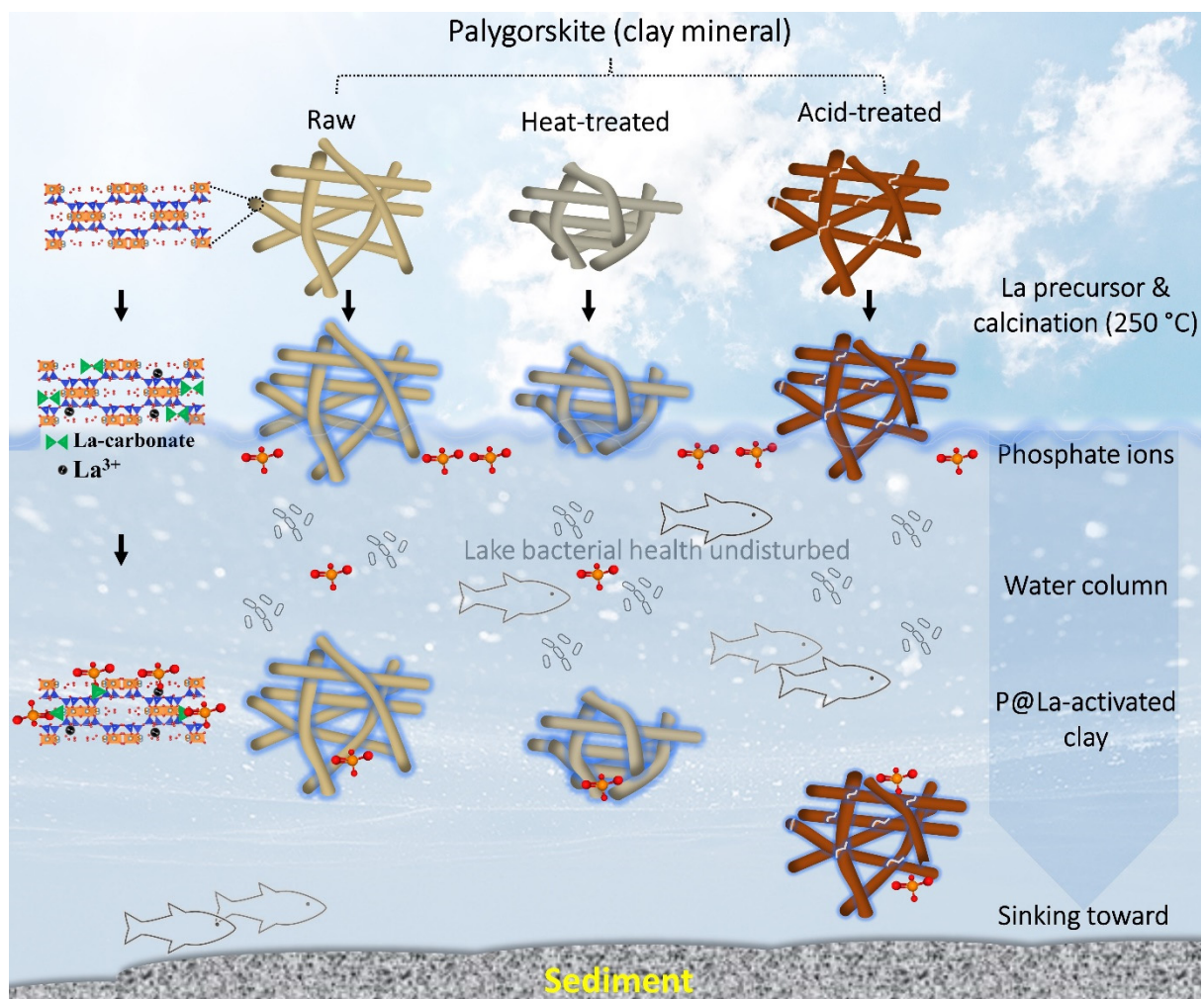


Figure 9. The overall modus operandi of the modified palygorskite in the lake water to remove phosphorus from surface water of the affected lake. The cartoon shows that La modified acid-treated palygorskite was efficient to adsorb P while travelling down to the bottom of the lake without impacting microbial health in the water column.

Supplementary Materials: The following are available online at <https://www.mdpi.com/article/10.3390/pr9111960/s1>, Figure number has been cited in the main text. In brief, the following method, data or images are provided: the XRD and zeta potential characteristics of materials with and without calcination (S1), bacterial growth facility (S2), microscopic images and spectroscopy of raw clay (S3), XPS profile of O 1s and C 1s regions (S4), particle settling study (S5), and bacterial curve at the early phase (S6).

Author Contributions: Conceptualization, R.N. and B.B.; Formal Analysis, B.B.; Investigation, B.B.; Data Curation, B.B.; Writing—Original Draft Preparation, B.B.; Writing—Review & Editing, R.N.; Visualization, B.B.; Project Administration, R.N. and B.B.; Funding Acquisition, R.N. All authors have read and agreed to the published version of the manuscript.

Funding: This research received no external funding.

Institutional Review Board Statement: Not applicable.

Informed Consent Statement: Not applicable.

Data Availability Statement: All results derived from original data are provided either in the main text or supplementary file.

Acknowledgments: We thank CRC CARE for financial support (grant no. care 6.47.01). We also acknowledge Microscopy Australia for facilities support (XPS, TEM and SEM-EDS) located at Future Industries Institute, University of South Australia.

Conflicts of Interest: The material described in this manuscript as lanthanum modified acid-treated Australian palygorskite has been filed as an Australian provisional patent, AusPat No. 2021902600.

References

1. Wigginton, N.S. Fertilizing water contamination. *Science* **2015**, *349*, 1297–1298. [[CrossRef](#)]
2. Zhao, C.; Shao, N.; Yang, S.; Ren, H.; Ge, Y.; Feng, P.; Dong, B.; Zhao, Y. Predicting cyanobacteria bloom occurrence in lakes and reservoirs before blooms occur. *Sci. Total Environ.* **2019**, *670*, 837–848. [[CrossRef](#)] [[PubMed](#)]
3. Moharami, S.; Jalali, M. Use of modified clays for removal of phosphorus from aqueous solutions. *Environ. Monit. Assess.* **2015**, *187*, 639. [[CrossRef](#)]
4. Xie, J.; Wang, Z.; Lu, S.; Wu, D.; Zhang, Z.; Kong, H. Removal and recovery of phosphate from water by lanthanum hydroxide materials. *Chem. Eng. J.* **2014**, *254*, 163–170. [[CrossRef](#)]
5. Razanajatovo, M.R.; Gao, W.; Song, Y.; Zhao, X.; Sun, Q.; Zhang, Q. Selective adsorption of phosphate in water using lanthanum-based nanomaterials: A critical review. *Chin. Chem. Lett.* **2021**, *32*, 2637–2647. [[CrossRef](#)]
6. Herrmann, H.; Nolde, J.; Berger, S.; Heise, S. Aquatic ecotoxicity of lanthanum—A review and an attempt to derive water and sediment quality criteria. *Ecotoxicol. Environ. Saf.* **2016**, *124*, 213–238. [[CrossRef](#)] [[PubMed](#)]
7. Van Oosterhout, F.; Goitom, E.; Roessink, I.; Lürling, M. Lanthanum from a Modified Clay Used in Eutrophication Control Is Bioavailable to the Marbled Crayfish (*Procambarus fallax f. virginalis*). *PLoS ONE* **2014**, *9*, e102410. [[CrossRef](#)] [[PubMed](#)]
8. Spears, B.M.; Lürling, M.; Yasseri, S.; Castro-Castellon, A.T.; Gibbs, M.; Meis, S.; McDonald, C.; McIntosh, J.; Sleep, D.; Van Oosterhout, F. Lake responses following lanthanum-modified bentonite clay (Phoslock®) application: An analysis of water column lanthanum data from 16 case study lakes. *Water Res.* **2013**, *47*, 5930–5942. [[CrossRef](#)] [[PubMed](#)]
9. Mucci, M.; Douglas, G.; Lürling, M. Lanthanum modified bentonite behaviour and efficiency in adsorbing phosphate in saline waters. *Chemosphere* **2020**, *249*, 126131. [[CrossRef](#)]
10. Castro, L.F.d.; Brandão, V.S.; Bertolino, L.C.; Souza, W.F.L.d.; Teixeira, V.G. Phosphate Adsorption by Montmorillonites Modified with Lanthanum/Iron and a Laboratory Test using Water from the Jacarepaguá Lagoon (RJ, Brazil). *J. Braz. Chem. Soc.* **2019**, *30*, 641–657. [[CrossRef](#)]
11. Kong, L.; Tian, Y.; Li, N.; Liu, Y.; Zhang, J.; Zhang, J.; Zuo, W. Highly-effective phosphate removal from aqueous solutions by calcined nano-porous palygorskite matrix with embedded lanthanum hydroxide. *Appl. Clay Sci.* **2018**, *162*, 507–517. [[CrossRef](#)]
12. Yin, H.; Yang, P.; Kong, M.; Li, W. Use of lanthanum/aluminum co-modified granulated attapulgite clay as a novel phosphorus (P) sorbent to immobilize P and stabilize surface sediment in shallow eutrophic lakes. *Chem. Eng. J.* **2020**, *385*, 123395. [[CrossRef](#)]
13. Guggenheim, S.; Kreckler, M.P.S. The Structures and Microtextures of the Palygorskite–Sepiolite Group Minerals. In *Developments in Clay Science*; Galán, E., Singer, A., Eds.; Elsevier: Amsterdam, The Netherlands, 2011; Volume 3, pp. 3–32.
14. Biswas, B.; Sarkar, B.; Naidu, R. Bacterial mineralization of phenanthrene on thermally activated palygorskite: A ¹⁴C radiotracer study. *Sci. Total Environ.* **2017**, *579*, 709–717. [[CrossRef](#)] [[PubMed](#)]
15. Biswas, B.; Sarkar, B.; Rusmin, R.; Naidu, R. Mild acid and alkali treated clay minerals enhance bioremediation of polycyclic aromatic hydrocarbons in long-term contaminated soil: A ¹⁴C-tracer study. *Environ. Pollut.* **2017**, *223*, 255–265. [[CrossRef](#)]
16. Melo, D.M.A.; Ruiz, J.A.C.; Melo, M.A.F.; Sobrinho, E.V.; Martinelli, A.E. Preparation and characterization of lanthanum palygorskite clays as acid catalysts. *J. Alloy. Compd.* **2002**, *344*, 352–355. [[CrossRef](#)]
17. Rakhimova, N.; Rakhimov, R. Advances in development of calcined clays as supplementary cementitious materials. *IOP Conf. Series Mater. Sci. Eng.* **2020**, *890*, 012085. [[CrossRef](#)]
18. Link, D.D.; Walter, P.J.; Kingston, H.M. Development and Validation of the New EPA Microwave-Assisted Leach Method 3051A. *Environ. Sci. Technol.* **1998**, *32*, 3628–3632. [[CrossRef](#)]
19. Degen, T.; Sadki, M.; Bron, E.; König, U.; Nénert, G. The HighScore suite. *Powder Diffr.* **2014**, *29*, S13–S18. [[CrossRef](#)]
20. Walton, J.; Wincott, P.; Fairley, N.; Carrick, A. *Peak Fitting with CasaXPS: A Casa Pocket Book*; Acolyte Science: Salisbury, UK, 2010; p. 132.
21. Pepper, I.L.; Gerba, C.P. Cultural Methods. In *Environmental Microbiology*, 2nd ed.; Maier, R.M., Ian, L.P., Charles, P.G., Eds.; Academic Press: San Diego, CA, USA, 2009; pp. 173–189.
22. Torfs, E.; Nopens, I.; Winkler, M.K.H.; Vanrolleghem, P.A.; Balemans, S.; Smets, I.Y. Settling tests. In *Experimental Methods in Wastewater Treatment*; Loosdrecht, M.C.M.v., Nielsen, P.H., Lopez-Vazquez, C.M., Brdjanovic, D., Eds.; IWA Publishing: London, UK, 2016; pp. 235–262.
23. Biswas, B.; Sarkar, B.; Naidu, R. Influence of thermally modified palygorskite on the viability of polycyclic aromatic hydrocarbon-degrading bacteria. *Appl. Clay Sci.* **2016**, *134*, 153–160. [[CrossRef](#)]
24. Chen, T.; Liu, H.; Li, J.; Chen, D.; Chang, D.; Kong, D.; Frost, R.L. Effect of thermal treatment on adsorption–desorption of ammonia and sulfur dioxide on palygorskite: Change of surface acid–alkali properties. *Chem. Eng. J.* **2011**, *166*, 1017–1021. [[CrossRef](#)]
25. España, V.A.A.; Sarkar, B.; Biswas, B.; Rusmin, R.; Naidu, R. Environmental applications of thermally modified and acid activated clay minerals: Current status of the art. *Environ. Technol. Innov.* **2019**, *13*, 383–397. [[CrossRef](#)]

26. Dithmer, L.; Lipton, A.; Reitzel, K.; Warner, T.E.; Lundberg, D.; Nielsen, U.G. Characterization of Phosphate Sequestration by a Lanthanum Modified Bentonite Clay: A Solid-State NMR, EXAFS, and PXRD Study. *Environ. Sci. Technol.* **2015**, *49*, 4559–4566. [[CrossRef](#)] [[PubMed](#)]
27. Kuroki, V.; Bosco, G.E.; Fadini, P.; Mozeto, A.A.; Cestari, A.R.; Carvalho, W.A. Use of a La(III)-modified bentonite for effective phosphate removal from aqueous media. *J. Hazard. Mater.* **2014**, *274*, 124–131. [[CrossRef](#)] [[PubMed](#)]
28. Xavier, K.C.M.; Santos, M.R.; Oliveira, M.E.R.; Carvalho, M.W.N.C.; Osajima, J.; Filho, E.C.D.S. Effects of acid treatment on the clay palygorskite: XRD, surface area, morphological and chemical composition. *Mater. Res.* **2014**, *17*, 3–8. [[CrossRef](#)]
29. García-Sánchez, J.J.; Solache-Ríos, M.; Martínez-Gutiérrez, J.M.; Arteaga-Larios, N.V.; Ojeda-Escamilla, M.C.; Rodríguez-Torres, I. Modified natural magnetite with Al and La ions for the adsorption of fluoride ions from aqueous solutions. *J. Fluor. Chem.* **2016**, *186*, 115–124. [[CrossRef](#)]
30. ThermoScientific. Lanthanum. Available online: <https://xpssimplified.com/elements/lanthanum.php> (accessed on 6 May 2021).
31. Li, J.P.H.; Zhou, X.; Pang, Y.; Zhu, L.; Vovk, E.I.; Cong, L.; van Bavel, A.P.; Li, S.; Yang, Y. Understanding of binding energy calibration in XPS of lanthanum oxide by in situ treatment. *Phys. Chem. Chem. Phys.* **2019**, *21*, 22351–22358. [[CrossRef](#)] [[PubMed](#)]
32. Langmuir, I. The constitution and fundamental properties of solids and liquids. Part I. Solids. *J. Am. Chem. Soc.* **1916**, *38*, 2221–2295. [[CrossRef](#)]
33. Freundlich, H. Über die Adsorption in Lösungen. *Z. Für Phys. Chem.* **1907**, *57U*, 385–470. [[CrossRef](#)]
34. Tran, H.N.; You, S.-J.; Hosseini-Bandegharai, A.; Chao, H.-P. Mistakes and inconsistencies regarding adsorption of contaminants from aqueous solutions: A critical review. *Water Res.* **2017**, *120*, 88–116. [[CrossRef](#)]
35. Wang, J.; Guo, X. Adsorption isotherm models: Classification, physical meaning, application and solving method. *Chemosphere* **2020**, *258*, 127279. [[CrossRef](#)]
36. Zhang, L.; Liu, Y.; Wang, Y.; Li, X.; Wang, Y. Investigation of phosphate removal mechanisms by a lanthanum hydroxide adsorbent using p-XRD, FTIR and XPS. *Appl. Surf. Sci.* **2021**, *557*, 149838. [[CrossRef](#)]
37. Wu, D.; Tian, S.; Long, J.; Peng, S.; Xu, L.; Sun, W.; Chu, H. Remarkable phosphate recovery from wastewater by a novel Ca/Fe composite: Synergistic effects of crystal structure and abundant oxygen-vacancies. *Chemosphere* **2021**, *266*, 129102. [[CrossRef](#)] [[PubMed](#)]